

This is the peer reviewed version of the following article:

Banister, S., Adams, A., Kevin, R., Macdonald, C., Glass, M., Boyd, R., Connor, M., McGregor, I., Havel, C., Bright, S., Vilamala, M., Lladanosa, C., Barratt, M. J., & Gerona, R. (2019). Synthesis and pharmacology of new psychoactive substance 5F-CUMYL-P7AICA, a scaffold- hopping analog of synthetic cannabinoid receptor agonists 5F-CUMYL-PICA and 5F-CUMYL-PINACA. *Drug Testing and Analysis*, 11(2), 279–291.

which has been published in final form at <https://doi.org/10.1002/dta.2491>

This article may be used for non-commercial purposes in accordance with [Wiley Terms and Conditions for Use of Self-Archived Versions](#).

© 2018. This manuscript version is made available under the CC-BY-NC-ND 4.0 license <http://creativecommons.org/licenses/by-nc-nd/4.0/>



Synthesis and pharmacology of synthetic cannabinoid 5F-CUMYL-P7AICA, a scaffold hopping analogue of 5F-CUMYL-PICA and 5F-CUMYL-PINACA

Journal:	<i>Drug Testing and Analysis</i>
Manuscript ID	DTA-18-0047.R2
Wiley - Manuscript type:	Research Article
Date Submitted by the Author:	n/a
Complete List of Authors:	Banister, Samuel; Stanford University, Department of Pathology Adams, Axel; University of California, San Francisco, Clinical Toxicology and Environmental Biomonitoring Laboratory Kevin, Richard; School of Psychology Macdonald, Christa; The University of Auckland, School of Medical Sciences Glass, Michelle; The University of Auckland, School of Medical Sciences Boyd, Rochelle; Macquarie University Faculty of Medicine and Health Sciences Connor, Mark; Macquarie University Faculty of Medicine and Health Sciences McGregor, Iain; The University of Sydney, School of Psychology Havel, Christopher; University of California, San Francisco, Department of Clinical Pharmacology Bright, Stephen; Edith Cowan University, School of Medical and Health Science; Curtin University National Drug Research Institute, Faculty of Health Sciences Ventura, Mireia; Energy control barcelona Gil, Cristina; Energy control barcelona Barratt, Monica; UNSW, National Drug and Alcohol Research Centre; Curtin University National Drug Research Institute, Faculty of Health Sciences; Burnet Institute, Behaviours and Health Risks Program Gerona, Roy; University of California, San Francisco, Clinical Toxicology and Environmental Biomonitoring Laboratory
Keywords:	cannabinoid, CUMYL, PINACA, P7AICA, mass spectrometry, pharmacology, scaffold hopping, biotelemetry
Abstract:	Synthetic cannabinoid receptor agonists (SCRAs) are a dynamic class of new psychoactive substances (NPS), with novel chemotypes emerging each year. Following the detection of 5F-CUMYL-P7AICA in Australia in 2016, the scaffold hopping SCRAs 5F-CUMYL-PICA, 5F-CUMYL-PINACA, 5F-CUMYL-P7AICA were synthesized and characterized by nuclear magnetic resonance (NMR) spectroscopy, gas chromatography–mass spectrometry (GC–MS), and liquid chromatography–quadrupole time-of-flight–MS (LC–QTOF–MS). Since little is known of the pharmacology of 7-azaindole SCRAs like 5F-CUMYL-P7AICA, the binding affinities and functional activities of all compounds at cannabinoid type 1 and type 2 receptors (CB1 and CB2

1
2
3
4
5
6
7
8
9
10
11
12
13
14
15
16
17
18
19
20
21
22
23
24
25
26
27
28
29
30
31
32
33
34
35
36
37
38
39
40
41
42
43
44
45
46
47
48
49
50
51
52
53
54
55
56
57
58
59
60

	respectively) were assessed using tritiated radioligand competition experiments and fluorescence-based plate reader membrane potential assays. Despite CB1 binding affinities differing by over two order of magnitude ($K_i = 2.95\text{--}174\text{ nM}$), all compounds were potent and efficacious CB1 agonists ($EC_{50} = 0.43\text{--}4.7\text{ nM}$), with consistent rank order for binding and functional activity (5F-CUMYL-PINACA > 5F-CUMYL-PICA > 5F-CUMYL-P7AICA). Additionally, 5F-CUMYL-P7AICA was found to exert potent cannabimimetic effects in mice, inducing hypothermia ($6\text{ }^\circ\text{C}$, 3 mg/kg) through a CB1-dependent mechanism.
--	--

SCHOLARONE™
Manuscripts

For Peer Review

1
2
3 **Synthesis and pharmacology of new psychoactive substance 5F-CUMYL-P7AICA, a**
4 **scaffold hopping analogue of synthetic cannabinoid receptor agonists 5F-CUMYL-PICA**
5
6 **and 5F-CUMYL-PINACA**
7
8
9
10
11

12 Samuel D. Banister,^{a*} Axel Adams,^b Richard C. Kevin,^c Christa Macdonald,^d Michelle Glass,^d
13 Rochelle Boyd,^e Mark Connor,^e Iain S. McGregor,^c Christopher M. Havel,^f Stephen J. Bright,^{g,h}
14 Mireia Ventura,ⁱ Cristina Gil,ⁱ Monica J. Barratt,^{j,h,k} and Roy R. Gerona^b
15
16
17
18
19
20

21 ^aDepartment of Pathology, Stanford University School of Medicine, Stanford, CA 94305, USA;

22 ^bClinical Toxicology and Environmental Biomonitoring Laboratory, University of California,
23
24 San Francisco, CA 94143, USA; ^cSchool of Psychology, The University of Sydney, Sydney,
25
26 NSW 2006, Australia; ^dSchool of Medical Sciences, The University of Auckland, Auckland,
27
28 New Zealand; ^eFaculty of Medicine and Health Sciences, Macquarie University, NSW 2109,
29
30 Australia; ^fDepartment of Clinical Pharmacology, University of California, San Francisco, CA
31
32 94143, USA; ^gSchool of Medical and Health Science, Edith Cowan University, Joondalup,
33
34 Australia; ^hNational Drug Research Institute, Faculty of Health Sciences, Curtin University,
35
36 Perth, Australia; ⁱEnergy Control, Asociación Bienestar y Desarrollo, Spain; ^jDrug Policy
37
38 Modelling Program, National Drug and Alcohol Research Centre, UNSW, Sydney, NSW,
39
40 Australia; ^kBehaviours and Health Risks Program, Burnet Institute, Melbourne, VIC, Australia
41
42
43
44
45
46
47
48

49 *Corresponding author
50
51
52
53
54
55
56
57
58
59
60

1
2
3 **Abstract:** Synthetic cannabinoid receptor agonists (SCRAs) are a dynamic class of new
4 psychoactive substances (NPS), with novel chemotypes emerging each year. Following the
5 putative detection of 5F-CUMYL-P7AICA in Australia in 2016, the scaffold hopping SCRAs
6 5F-CUMYL-PICA, 5F-CUMYL-PINACA, 5F-CUMYL-P7AICA were synthesized and
7 characterized by nuclear magnetic resonance (NMR) spectroscopy, gas chromatography–mass
8 spectrometry (GC–MS), and liquid chromatography–quadrupole time-of-flight–MS (LC–QTOF–
9 MS). Since little is known of the pharmacology of 7-azaindole SCRAs like 5F-CUMYL-
10 P7AICA, the binding affinities and functional activities of all compounds at cannabinoid type 1
11 and type 2 receptors (CB₁ and CB₂, respectively) were assessed using tritiated radioligand
12 competition experiments and fluorescence-based plate reader membrane potential assays.
13 Despite CB₁ binding affinities differing by over two orders of magnitude ($K_i = 2.95\text{--}174$ nM), all
14 compounds were potent and efficacious CB₁ agonists ($EC_{50} = 0.43\text{--}4.7$ nM), with consistent rank
15 order for binding and functional activity (5F-CUMYL-PINACA > 5F-CUMYL-PICA > 5F-
16 CUMYL-P7AICA). Additionally, 5F-CUMYL-P7AICA was found to exert potent
17 cannabimimetic effects in mice, inducing hypothermia (6 °C, 3 mg/kg) through a CB₁-dependent
18 mechanism.

19
20
21
22
23
24
25
26
27
28
29
30
31
32
33
34
35
36
37
38
39
40
41
42 **Keywords:** cannabinoid, CUMYL, PINACA, P7AICA, scaffold hopping, mass spectrometry,
43 pharmacology, biotelemetry
44
45
46
47
48
49
50
51
52
53
54
55
56
57
58
59
60

1
2
3 **Introduction:** More than 230 synthetic cannabinoid receptor agonists (SCRAs) have been
4 reported to the United Nations Office on Drugs and Crime (UNODC) as recreational drugs,¹
5 representing the largest and most structurally diverse class of new psychoactive substances
6 (NPS). The structural heterogeneity of SCRAs has increased since the first examples were
7 identified in 2008, and novel chemotypes continue to emerge in an attempt to circumvent
8 structure-based prohibition.² The earliest examples, such as 1-alkyl-3-acylindole JWH-018 (**1**,
9 Figure 1), were repurposed from tool molecules described by John W. Huffman at Clemson
10 University for studying cannabinoid receptors. Since then, many SCRAs with no precedent in the
11 chemical literature, e.g. APICA (**2**) and BB-22 (**3**), have been reported. Most recently, SCRAs
12 derived from a series of pharmaceutical patents (e.g. AMB-FUBINACA, **4**) have been associated
13 with serious adverse reactions.³

14
15
16
17
18
19
20
21
22
23
24
25
26
27
28
29
30
31 [APPROXIMATE PLACEMENT OF FIGURE 1]
32
33
34

35 One class of SCRAs increasingly identified by forensic scientists and clinical toxicologists are
36 heteroaromatic carboxamides containing a pendant cumylamine group.⁴⁻⁷ The Slovenian
37 National Focal Point notified the identification of 5F-CUMYL-PICA (**5**) through the European
38 Monitoring Center for Drugs and Drug Addiction (EMCDDA) early warning system (EWS) on
39 23 September 2014.⁸ The indazole analogue of 5F-CUMYL-PICA, 5F-CUMYL-PINACA (**6**),
40 was notified by the Swedish EWS participants several weeks later.⁸ These compounds were
41 previously reported in a 2014 patent as SGT-67 and SGT-25, respectively.⁹ Unexpectedly, 5F-
42 CUMYL-P7AICA (**7**), containing a 7-azaindole (pyrrolo[2,3-*b*]pyridine) core rather than an
43 indole or indazole, was notified to the EWS in February 2015.¹⁰ 5F-CUMYL-P7AICA does not
44
45
46
47
48
49
50
51
52
53
54
55
56
57
58
59
60

1
2
3 appear in patent WO2014167530 or elsewhere in historical chemical literature, and may be the
4
5 product of rational design by unknown parties.
6
7
8
9

10 In October 2016, legislation was implemented in Victoria, Australia to restrict SCRA products
11
12 by prohibiting several structural classes, including indole- and indazole-3-carboxamides.
13
14 However, by November 2016 new putative SCRA products were available, and a product
15
16 branded "Rasta King" (Fig. 2a) was obtained by test purchase for the purpose of analysis. Gas
17
18 chromatography-mass spectrometry (GC-MS) putatively identified 5F-CUMYL-P7AICA by
19
20 comparison of GC retention time (total ion chromatogram, TIC) and MS fragmentation spectrum
21
22 (Fig. 2b) with several public spectral libraries, and the internal mass spectral library of Energy
23
24 Control. Comparison of the sample EI-MS spectrum to a spectral library cannot exclude certain
25
26 structural isomers, however, neither 5F-CUMYL-P7AICA nor its regioisomers have been
27
28 formally detected in Australia to date. This prompted us to characterize the chemistry and
29
30 pharmacology of 5F-CUMYL-P7AICA and its scaffold hopping analogs 5F-CUMYL-PICA and
31
32 5F-CUMYL-PINACA, all of which have been previously detected in other parts of the world.
33
34
35
36
37
38
39

40 [APPROXIMATE PLACEMENT OF FIGURE 2]
41
42
43

44 Scaffold hopping is the technique of modifying the central core of a bioactive molecule to
45
46 improve activity, and is commonly used by medicinal chemists during the drug discovery
47
48 process.^{11,12} 5F-CUMYL-P7AICA is the first example of a pyrrolo[2,3-*b*]pyridine SCRA
49
50 discovered as a putative NPS, and one of few reported examples of clandestine scaffold hopping.
51
52 In this case, incorporation of a pyrrolo[2,3-*b*]pyridine core was possibly inspired by the
53
54
55
56
57
58
59
60

1
2
3 cannabinoid activity of azaindoles previously reported by pharmaceutical scientists,¹³ and may
4 represent an attempt to circumvent structure-based legislative changes.
5
6
7

8
9
10 SCRAAs featuring pyrrolo[2,3-*b*]pyridine cores and other bicyclic heteroaromatic scaffolds
11 continue to be reported,¹⁴⁻¹⁶ and little is known about their pharmacology and toxicology.^{7,17-20}
12
13

14 We prepared **5**, **6**, and **7**, and investigated methods for discrimination of these analogues using
15 nuclear magnetic resonance (NMR) spectroscopy, gas chromatograph–mass spectrometry (GC–
16 MS), and liquid chromatography–quadrupole time-of-flight–MS (LC–QTOF–MS). Additionally,
17 we determined the binding affinities and functional activities of **5**, **6**, and **7**, at human CB₁ and
18 CB₂ receptors *in vitro*. Having previously described the cannabinoid activity of several
19 cumylamine SCRAAs *in vivo*, we used mouse biotelemetry to rank the relative potency of **7**
20 compared to **5** and **6** in a living system.
21
22
23
24
25
26
27
28
29
30

31 32 33 **Experimental.**

34
35 **General chemical synthesis details.** All reactions were performed under an atmosphere of
36 nitrogen or argon unless otherwise specified. Anhydrous dichloromethane, *N,N*-
37 dimethylformamide (DMF), methanol, and toluene were used as purchased. All other
38 commercially available reagents (Sigma-Aldrich) were used as purchased. Analytical thin layer
39 chromatography (TLC) was performed using Merck aluminum-backed silica gel 60 F254 (0.2
40 mm) plates which were visualized using shortwave (254 nm) ultra-violet fluorescence. Flash
41 chromatography was performed using Merck Kieselgel 60 (230–400 mesh) silica gel. Melting
42 points were measured in open capillaries using a Laboratory Devices Mel-Temp II and are
43 uncorrected. Nuclear magnetic resonance spectra were recorded at 298 K using an Agilent 400
44
45
46
47
48
49
50
51
52
53
54
55
56
57
58
59
60

MHz spectrometer. The data are reported as chemical shift (δ ppm) relative to the residual protonated solvent resonance, relative integral, multiplicity (s = singlet, br s = broad singlet, d = doublet, t = triplet, q = quartet, quin. = quintet, sep = septet, m = multiplet), coupling constants (J Hz) and assignment. Assignment of signals was assisted by COSY, DEPT, HSQC, and HMBC experiments where necessary. Fourier-transform infrared (FTIR) spectroscopy data were previously reported for these compounds, with no remarkable spectral differences noted.¹⁵

1-(5-Fluoropentyl)-*N*-(2-phenylpropan-2-yl)-1*H*-indole-3-carboxamide (5). A solution of 1-(5-fluoropentyl)-1*H*-indole-3-carboxylic acid (**10**, 63 mg, 0.25 mmol) in CH₂Cl₂ (2.5 mL) was treated with (COCl)₂ (45 μ L, 0.5 mmol, 2.0 equiv.) followed by DMF (1 drop). After stirring for 2 h, the solution was evaporated *in vacuo*, and the crude acid chloride was used immediately in the following step.

A cooled (0 °C) solution of the freshly prepared acid chloride (0.25 mmol) in CH₂Cl₂ (2.5 mL) was treated with Et₃N (88 μ L, 0.63 mmol, 2.5 equiv.) and cumylamine (44 μ L, 0.3 mmol, 1.2 equiv.), and stirred at ambient temperature for 14 h. The mixture was partitioned between CH₂Cl₂ (10 mL) and 1 M aq. HCl (5 mL). The layers were separated and the organic phase was washed with 1 M aq. HCl (2 \times 5 mL), sat. aq. NaHCO₃ (3 \times 5 mL), brine (5 mL), dried (MgSO₄), and the solvent evaporated under reduced pressure. Following recrystallization from *i*-PrOH, **5** was obtained as fine white needles (72 mg, 78%). R_f 0.37 (hexane-EtOAc, 50:50); m.p. 193–195 °C; ¹H NMR (400 MHz, CDCl₃): δ 7.92–7.90 (1H, m, ArH), 7.69 (1H, s, ArH), 7.53–7.50 (2H, m, ArH), 7.40–7.33 (3H, m, ArH), 7.30–7.22 (3H, m, ArH), 6.28 (1H, s, NH), 4.42 (2H, dt, J = 47.2, 6.0 Hz, CH₂F), 4.15 (2H, t, J = 7.2 Hz, NCH₂), 1.91 (2H, quin., J = 7.8 Hz,

1
2
3 CH₂), 1.87 (6H, s, 2 × CH₃), 1.77-1.64 (2H, m, CH₂), 1.49-1.41 (2H, m, CH₂); ¹³C NMR (100
4 MHz, CDCl₃): δ 164.4 (CO), 147.5 (quat.), 136.7 (quat.), 131.8 (CH), 128.6 (CH), 126.7 (CH),
5
6 125.3 (quat.), 125.0 (CH), 122.5 (CH), 121.5 (CH), 120.0 (CH), 112.0 (quat.), 110.4 (CH), 83.8
7
8 (d, ¹J_{CF} = 165.0 Hz, CH₂F), 56.2 (quat.), 46.8 (CH₂), 30.1 (d, ²J_{CF} = 19.9 Hz, CH₂), 29.8 (2 ×
9
10 CH₃), 29.8 (CH₂), 23.0 (d, ³J_{CF} = 4.9 Hz, CH₂).

11
12
13
14
15
16
17 **General procedure for amidation of 1-(5-fluoropentyl)-1H-indazole-3-carboxylic acid and**
18
19 **1-(5-fluoropentyl)-1H-pyrrolo[2,3-b]pyridine-3-carboxylic acid.** To a solution of 1-(5-
20 fluoropentyl)-1H-indazole-3-carboxylic acid or 1-(5-fluoropentyl)-1H-pyrrolo[2,3-b]pyridine-3-
21 carboxylic acid (0.25 mmol) in DMF (1.25 mL) was added HOBt·H₂O (42 mg, 0.28 mmol, 1.1
22 equiv.), EDC·HCl (63 mg, 0.33 mmol, 1.3 equiv.), cumylamine (40 μL, 0.28 mmol, 1.1 equiv.),
23 and Et₃N (70 μL, 0.50 mmol, 2.0 equiv.), and the mixture stirred at ambient temperature for 14
24 h. The mixture was poured onto H₂O (60 mL), extracted with EtOAc (3 × 10 mL), and the
25 combined organic were washed with H₂O (2 × 10 mL), brine (10 mL), dried (MgSO₄), and the
26 solvent evaporated under reduced pressure. The crude products were purified by flash
27 chromatography.
28
29
30
31
32
33
34
35
36
37
38
39
40
41

42 **1-(5-Fluoropentyl)-N-(2-phenylpropan-2-yl)-1H-indazole-3-carboxamide (6).** Subjecting 1-
43 (5-fluoropentyl)-1H-indazole-3-carboxylic acid (**15**, 63 mg, 0.25 mmol) to the procedure above
44 gave, following purification by flash chromatography (hexane-EtOAc 70:30), **6** as a colorless
45 resin (75 mg, 82%). R_f 0.65 (hexane-EtOAc, 50:50); ¹H NMR (400 MHz, CDCl₃): δ 8.34 (1H,
46 dt, *J* = 8.2, 0.9 Hz, ArH), 7.53-7.50 (2H, m, ArH), 7.43-7.32 (5H, m, ArH, NH, overlapping),
47 7.26-7.20 (2H, m, ArH), 4.44 (2H, dt, *J* = 47.3, 6.0 Hz, CH₂F), 4.41 (2H, t, *J* = 7.1 Hz, NCH₂),
48
49
50
51
52
53
54
55
56
57
58
59
60

2.01 (2H, quin., $J = 7.6$ Hz, CH₂), 1.87 (6H, s, 2 × CH₃), 1.82-1.69 (2H, m, CH₂), 1.53-1.45 (2H, m, CH₂); ¹³C NMR (100 MHz, CDCl₃): δ 162.0 (CO), 147.4 (quat.), 141.0 (quat.), 138.0 (quat.), 128.6 (CH), 126.8 (CH), 126.7 (CH), 125.0 (CH), 123.4 (CH), 123.0 (quat.), 122.6 (CH), 109.1 (CH), 83.9 (d, ¹J_{CF} = 165.0 Hz, CH₂F), 55.9 (quat.), 49.3 (NCH₂), 30.1 (d, ²J_{CF} = 19.7 Hz, CH₂), 29.8 (2 × CH₃), 29.5 (CH₂), 22.9 (d, ³J_{CF} = 5.0 Hz, CH₂).

1-(5-Fluoropentyl)-N-(2-phenylpropan-2-yl)-1H-pyrrolo[2,3-*b*]pyridine-3-carboxamide (7, 5F-CUMYL-P7AICA). Subjecting 1-(5-fluoropentyl)-1H-pyrrolo[2,3-*b*]pyridine-3-carboxylic acid (**16**, 68 mg, 0.25 mmol) to the procedure above gave, following purification by flash chromatography (hexane-EtOAc 50:50), **7** as a white crystalline solid (74 mg, 81%). m.p. 174–176 °C; R_f 0.31 (hexane-EtOAc, 50:50); ¹H NMR (400 MHz, CDCl₃): δ 8.36 (1H, dd, $J = 4.7$, 1.6 Hz, ArH), 8.27 (1H, dd, $J = 8.0$, 1.6 Hz, ArH), 7.74 (1H, s, ArH), 7.52-7.49 (2H, m, ArH), 7.38-7.33 (2H, m, ArH), 7.27-7.23 (1H, m, ArH), 7.18 (1H, dd, $J = 8.0$, 4.7 Hz, ArH), 6.14 (1H, br s, NH), 4.42 (2H, dt, $J = 47.3$, 6.0 Hz, CH₂F, overlapped), 4.32 (2H, t, $J = 7.3$ Hz, NCH₂), 1.94 (2H, quin., $J = 7.5$ Hz, CH₂), 1.86 (6H, s, 2 × CH₃), 1.81-1.66 (2H, m, CH₂), 1.49-1.42 (2H, m, CH₂); ¹³C NMR (100 MHz, CDCl₃): δ 163.7 (CO), 147.8 (quat.), 147.3 (quat.), 143.9 (CH), 130.4 (CH), 128.9 (CH), 128.7 (CH), 126.8 (CH), 124.9 (CH), 118.3 (quat.), 117.5 (CH), 110.3 (quat.), 83.9 (d, ¹J_{CF} = 164.9 Hz, CH₂F), 56.3 (quat.), 45.0 (NCH₂), 30.1 (d, ²J_{CF} = 19.8 Hz, CH₂), 30.0 (CH₂), 29.7 (2 × CH₃), 22.8 (d, ³J_{CF} = 5.0 Hz, CH₂).

1-(5-Fluoropentyl)-1H-indole-3-carboxylic acid (10). To a cooled (0 °C) suspension of sodium hydride (60% dispersion in mineral oil, 120 mg, 3.00 mmol, 2.0 equiv.) in DMF (1.5 mL) was added dropwise a solution of indole (176 mg, 1.50 mmol) in DMF (0.2 mL) and the mixture

1
2
3 allowed to stir at ambient temperature for 10 min. The mixture was cooled (0 °C), treated
4 dropwise with the appropriate 1-bromo-5-fluoropentane (195 μ L, 1.58 mmol, 1.05 equiv.), and
5
6 stirred at ambient temperature for 1 h. The mixture was cooled (0 °C), treated portionwise with
7
8 trifluoroacetic anhydride (521 μ L, 3.75 mmol, 2.5 equiv.), and stirred at ambient temperature for
9
10 1 h. The solution was poured portionwise onto vigorously stirred ice-water (90 mL) until
11
12 precipitation was complete, and the formed red-pink solid was filtered and air dried overnight.
13
14
15
16
17
18

19 To a refluxing solution of potassium hydroxide (278 mg, 4.95 mmol, 3.3 equiv.) in methanol
20
21 (0.55 mL) was added portionwise a solution of the crude 1-(5-fluoropentyl)-3-trifluoroacetyl-1*H*-
22
23 indole (**9**, 452 mg, 1.50 mmol) in toluene (1.25 mL) and the solution heated at reflux for 2 h. The
24
25 solution was cooled to ambient temperature and partitioned between 1 M aq. NaOH (40 mL) and
26
27 Et₂O (5 mL). The layers were separated, and the aqueous layer was adjusted to pH 1 with 10 M
28
29 aq. HCl. The aqueous phase was extracted with Et₂O (3 \times 10 mL), dried (Na₂SO₄), and solvent
30
31 evaporated under reduced pressure. The crude product was recrystallized from *i*-PrOH and gave
32
33 **10** as a colorless crystalline solid (249 mg, 67% over 2 steps). m.p. 120–122 °C (lit. m.p. 120–
34
35 122 °C)²¹; ¹H NMR (400 MHz, CDCl₃): δ 8.29-8.25 (1H, m, ArH), 7.93 (1H, s, ArH), 7.41-7.37
36
37 (1H, m, ArH), 7.34-7.30 (2H, m, ArH), 4.43 (2H, dt, ²*J*_{HF} = 47.3, ³*J*_{HH} = 5.9 Hz, CH₂F), 4.18
38
39 (2H, t, *J* = 7.1 Hz, NCH₂), 1.95 (2H, quin., *J* = 7.1 Hz, CH₂), 1.78-1.68 (2H, m, CH₂), 1.52-1.44
40
41 (2H, m, CH₂); ¹³C NMR (100 MHz, CDCl₃): δ 170.9 (CO), 136.8 (quat.), 135.6 (CH), 127.1
42
43 (quat.), 123.0 (CH), 122.3 (CH), 122.1 (CH), 110.1 (CH), 106.6 (quat.), 83.8 (d, ¹*J*_{CF} = 165.2 Hz,
44
45 CH₂F), 47.1 (CH₂), 30.0 (d, ²*J*_{CF} = 19.8 Hz, CH₂), 29.6 (CH₂), 22.9 (d, ³*J*_{CF} = 5.0 Hz, CH₂).
46
47
48
49
50
51
52
53
54
55
56
57
58
59
60

Methyl 1-(5-fluoropentyl)-1*H*-indazole-3-carboxylate (13). To a cooled (0 °C) solution of methyl 1*H*-indazole-3-carboxylate (**11**, 176 mg, 1.00 mmol, 1.0 equiv.) in THF (5.0 mL) was added dropwise a 1 M solution of potassium tert-butoxide in THF (1.1 mL, 1.1 mmol, 1.1 equiv.), and the solution stirred at ambient temperature for 1 h. The solution was cooled (0 °C), treated dropwise with 1-bromo-5-fluoropentane (130 μL, 1.05 mmol, 1.05 equiv.), and stirred at ambient temperature for 14 h. The mixture was partitioned between EtOAc (10 mL) and H₂O (30 mL) and the layers separated. The aqueous layer was extracted with EtOAc (3 × 10 mL), and the combined organic phases were washed with brine (10 mL), dried (Na₂SO₄), and the solvent evaporated under reduced pressure affording, following purification by flash chromatography (hexane-EtOAc, 85:15), **13** as a colorless oil (206 mg, 78%). *R*_f 0.51 (hexane-EtOAc, 80:20); ¹H NMR (400 MHz, CDCl₃): δ 8.24 (1H, dt, *J* = 8.2, 1.0 Hz), 7.49-7.42 (2H, m), 7.32 (1H, ddd, *J* = 8.2, 6.4, 1.4 Hz), 4.49 (2H, t, *J* = 7.2 Hz, NCH₂), 4.40 (2H, dt, ²*J*_{HF} = 47.3, ³*J*_{HH} = 6.0 Hz, CH₂F), 4.04 (3H, s, CH₃), 2.02 (2H, quin. *J* = 7.6 Hz, CH₂), 1.78-1.65 (2H, m, CH₂), 1.50-1.42 (2H, m, CH₂); ¹³C NMR (100 MHz, CDCl₃): δ 163.1 (CO), 140.5 (quat.), 134.6 (quat.), 126.9 (CH), 123.7 (quat.), 123.1 (CH), 122.3 (CH), 109.6 (CH), 83.6 (d, ¹*J*_{CF} = 165.0 Hz, CH₂F), 52.0 (CH₃), 49.7 (NCH₂), 29.9 (d, ²*J*_{CF} = 19.8 Hz, CH₂), 29.5 (CH₂), 22.7 (d, ³*J*_{CF} = 5.2 Hz, CH₂).

Methyl 1-(5-fluoropentyl)-1*H*-pyrrolo[2,3-*b*]pyridine-3-carboxylate (14). A cooled (0 °C) solution of methyl 1*H*-pyrrolo[2,3-*b*]pyridine-3-carboxylate (**12**, 126 mg, 1.00 mmol) in DMF (5 mL) was treated portionwise with NaH (60% dispersion in mineral oil, 44 mg, 1.10 mmol, 1.1 equiv.) and stirred at ambient temperature for 1 h. The mixture was cooled (0 °C) and treated dropwise with 1-bromo-5-fluoropentane (178 mg, 1.05 mmol, 1.05 equiv.). After stirring at ambient temperature for 24 h, the mixture was poured onto H₂O (100 mL) and extracted with

1
2
3 EtOAc (3 × 15 mL). The combined organic extracts were washed with H₂O (2 × 15 mL), brine
4 (15 mL), dried (MgSO₄), and solvent evaporated under reduced pressure. The crude material was
5 purified by flash chromatography (hexane-EtOAc 50:50) to give **14** as a colorless oil (175 mg,
6 66%). R_f 0.43 (hexane-EtOAc, 50:50); ¹H NMR (400 MHz, CDCl₃): δ 8.41 (1H, dd, *J* = 7.9, 1.6
7 Hz, ArH), 8.37 (1H, dd, *J* = 4.7, 1.6 Hz, ArH), 7.94 (1H, s, ArH), 7.21 (1H, dd, *J* = 7.9, 4.7 Hz,
8 ArH), 4.41 (2H, dt, *J* = 47.3, 6.0 Hz, CH₂F, overlapped), 4.34 (2H, t, *J* = 7.2 Hz, NCH₂), 3.91
9 (3H, s, CH₃), 1.96 (2H, quin., *J* = 7.5 Hz, CH₂), 1.80-1.66 (2H, m, CH₂), 1.50-1.42 (2H, m,
10 CH₂); ¹³C NMR (100 MHz, CDCl₃): δ 165.1 (CO), 147.8 (quat.), 144.1 (CH), 134.1 (CH), 130.1
11 (CH), 119.2 (quat.), 118.1 (CH), 105.7 (quat.), 83.8 (d, ¹*J*_{CF} = 165.0 Hz, CH₂F), 51.3 (CH₃), 45.2
12 (NCH₂), 30.1 (d, ²*J*_{CF} = 19.8 Hz, CH₂), 29.9 (CH₂), 22.7 (d, ³*J*_{CF} = 5.2 Hz, CH₂).
13
14
15
16
17
18
19
20
21
22
23
24
25
26
27

28 **1-(5-Fluoropentyl)-1H-indazole-3-carboxylic acid (15)**. To a solution of **13** (198 mg, 0.75
29 mmol) in MeOH (7.5 mL) was added 1 M aq. NaOH (3.0 mL) in a single portion, and the
30 solution stirred at ambient temperature for 16 h. The solvent was evaporated under reduced
31 pressure, the crude material dissolved in H₂O (30 mL), and the pH adjusted to 2 with 10 M aq.
32 HCl. The aqueous phase was extracted with EtOAc (3 × 10 mL), and the combined organic
33 layers were washed with brine (5 mL), dried (Na₂SO₄), and the solvent evaporated under reduced
34 pressure to afford **15** as a white powder (185 mg, 98%). m.p. 80–82 °C; ¹H NMR (400 MHz,
35 CDCl₃): δ 8.27 (1H, dt, *J* = 8.2, 1.0 Hz, ArH), 7.52-7.46 (2H, m, ArH), 7.37 (1H, ddd, *J* = 8.2,
36 6.2, 1.7 Hz, ArH), 4.52 (2H, t, *J* = 7.2 Hz, NCH₂), 4.43 (2H, dt, *J* = 47.3, 6.0 Hz, CH₂F), 2.06
37 (2H, quin., *J* = 7.6 Hz, CH₂), 1.81-1.67 (2H, m, CH₂), 1.52-1.44 (2H, m, CH₂); ¹³C NMR (100
38 MHz, CDCl₃): δ 166.4 (CO), 141.0 (quat.), 134.1 (quat.), 127.2 (CH), 124.0 (CH), 123.7 (CH),
39
40
41
42
43
44
45
46
47
48
49
50
51
52
53
54
55
56
57
58
59
60

1
2
3 122.5 (quat.), 109.8 (CH), 83.8 (d, $^1J_{CF} = 165.0$ Hz, CH₂F), 50.0 (NCH₂), 30.1 (d, $^2J_{CF} = 19.8$ Hz,
4
5 CH₂), 29.5 (CH₂), 22.9 (d, $^3J_{CF} = 5.0$ Hz, CH₂).
6
7
8
9

10 **1-(5-Fluoropentyl)-1H-pyrrolo[2,3-b]pyridine-3-carboxylic acid (16).** A solution of **14** (175
11 mg, 0.66 mmol) in MeOH (8 mL) was treated with 1 M aq. NaOH (4 mL, 4 mmol, 6 equiv.) and
12 stirred at ambient temperature for 96 h. The solvent was evaporated under reduced pressure and
13 the crude material added to H₂O (15 mL). The solution was adjusted to pH 2 with 10 M aq. HCl,
14 and the aqueous phase was extracted with CHCl₃ (3 × 15 mL). The combined organic extracts
15 were dried (MgSO₄) and the solvent evaporated under reduced pressure to give **16** (155 mg,
16 94%) as a white solid. m.p. 143–145 °C; ¹H NMR (400 MHz, CDCl₃): δ 8.48 (1H, dd, $J = 7.9$,
17 1.6 Hz, ArH), 8.42 (1H, dd, $J = 4.7$, 1.6 Hz, ArH), 8.05 (1H, s, ArH), 7.26 (1H, dd, $J = 7.9$, 4.7
18 Hz, ArH), 4.43 (2H, dt, $J = 47.3$, 6.0 Hz, overlapped, CH₂F), 4.38 (2H, t, $J = 7.2$ Hz, NCH₂),
19 1.99 (2H, quin., $J = 7.5$ Hz, CH₂), 1.80-1.70 (2H, m, CH₂), 1.53-1.47 (2H, m, CH₂); ¹³C NMR
20 (100 MHz, CDCl₃): δ 169.6 (CO), 148.0 (quat.), 144.3 (CH), 135.3 (CH), 130.3 (CH), 119.5
21 (quat.), 118.4 (CH), 105.1 (quat.), 83.8 (d, $^1J_{CF} = 165.0$ Hz, CH₂F), 45.4 (NCH₂), 30.1 (d, $^2J_{CF} =$
22 19.8 Hz, CH₂), 29.9 (CH₂), 22.8 (d, $^3J_{CF} = 5.1$ Hz, CH₂).
23
24
25
26
27
28
29
30
31
32
33
34
35
36
37
38
39
40
41

42 **GC-MS analysis method for herbal product obtained by test purchase.** A portion of the
43 “Rasta King” SCRA herbal product (24.2 mg) obtained by test purchase was dissolved in 10 mL
44 of methanol in a glass vial, sonicated for 15 minutes, and centrifuged for 10 min at 3500 rpm.
45 The supernatant was analyzed using gas chromatography–mass spectrometry (GC-MS) on an
46 Agilent 7890B gas chromatograph coupled to a 5977A quadrupole mass spectrometer detector
47 (Agilent; Santa Clara, CA, USA). The gas chromatograph was fitted with a G4513A auto-
48
49
50
51
52
53
54
55
56
57
58
59
60

1
2
3 sampler injector. Insert liners packed with silanized glasswool were used, and the injector and
4 the interface were operated at 280 °C. One μL of sample was injected in split mode, with a split
5 ratio 1:10, into a 20 m, 0.18 mm i.d., 0.18 μm film thickness 5% phenylmethylsilicone column
6 (HP-5MS UI-1909S-577UI, Fast type, Agilent Technologies). Helium was used as carrier gas at
7 a flow rate of 0.6 mL/min. The oven temperature was initially maintained at 90 °C and
8 programmed to reach 320 °C at 25 °C per min. It was finally maintained at 320 °C for 3 min
9 (total run time was 15.2 min). Subsequently a 3-minute post run at 320 °C. The mass
10 spectrometer was operated in electronic ionization mode at 70 eV. MS system worked in
11 SCAN acquisition mode, acquiring from m/z 40 to 400 Da. The obtained spectrum was compared
12 to the Searchable Mass Spectral Library NIST/EPA/NIH Mass Spectral Library, Data
13 Version: NIST 14; Searchable Mass Spectral Library Version 3.1
14 (<http://www.swgdrug.org/ms.htm>), Searchable Mass Spectral Library Cayman Spectral Library
15 (CSL) (<https://www.caymanchem.com/app/template/SpectralLibrary.vm>), European project
16 RESPONSE (http://www.policija.si/apps/nfl_response_web/seznam.php) and Energy Control's
17 internal mass spectral library.
18
19
20
21
22
23
24
25
26
27
28
29
30
31
32
33
34
35
36
37
38
39

40 **GC-MS analysis acquisition and analysis method for synthesized standards.** Synthetic
41 standards were dissolved to in methanol (10 $\mu\text{g}/\text{mL}$), and samples were analyzed using a Thermo
42 Scientific TRACE 1300 Series gas chromatograph coupled to a Thermo Scientific TSQ 8000
43 Evo Triple Quadrupole mass spectrometer system (Thermo Fisher Scientific, Waltham, MA,
44 USA). The injector and the interface were operated at 280 °C. One μL of sample were injected in
45 split mode, with a splitless, into a 30 m, 0.25 mm i.d., 0.18 μm film thickness 5%
46 phenylmethylsilicone column (HP-5MS UI-19091S-577UI, P/N 19091S-433 Agilent J&W
47
48
49
50
51
52
53
54
55
56
57
58
59
60

1
2
3 Technologies). Helium was used as carrier gas at a flow rate of 1.2 mL/min. The oven
4
5 temperature was ramped from 100 °C to 320 °C at 33.3 °C per min. It was maintained at 320 °C
6
7 for 5 min for a total run time of 11.6 min, followed by a 5 min post run at 320 °C. The mass
8
9 spectrometer was operated in electronic ionization mode at 70 eV. MS system worked in SCAN
10
11 acquisition mode, acquiring from m/z 40 to 400 Da.
12
13
14
15
16

17 **LC-QTOF/MS acquisition and analysis method for synthesized standards.** All samples were
18
19 analyzed using an Agilent LC 1260 Infinity Binary Liquid Chromatograph (LC) System attached
20
21 to an Agilent 6550 iFunnel Quadrupole Time-of-Flight Mass Spectrometer (QTOF/MS) 6550
22
23 (Agilent Technologies, Santa Clara, CA). An Agilent jet stream electrospray ionization (ESI)
24
25 source with a dual nebulizer that allows constant introduction of reference mass during sample
26
27 run was used to ionize sample organic components in positive mode.
28
29
30
31
32

33 Each sample was prepared from a crystalline aliquot of purified synthetic product and diluted to
34
35 a final concentration of 100 and 10 ng/mL in 10% LC-MS grade acetonitrile (Honeywell B&J,
36
37 Muskegon, MI); two concentrations were injected to elucidate potential solvent impurities or
38
39 instrument artifacts, and to ensure that similar fragmentation spectra are obtained at
40
41 concentrations relevant for the analysis of biological samples. In each sample run, 2.5 μ L was
42
43 injected into an Agilent Poroshell 120 C-18 column (2.1 \times 100 mm, 2.7 μ m) maintained at 50
44
45 °C. Chromatographic separation was achieved by gradient elution using LC-MS grade water
46
47 (Honeywell B&J, Muskegon, MI) with 0.05% formic acid and 5mM ammonium formate as
48
49 mobile phase A, and acetonitrile with 0.05% formic acid as mobile phase B. The elution gradient
50
51 used was 0–0.5 min = 5% B; 1.5 min = 30% B; 4.5 min = 70% B; 7.5 min = 100% B; 7.5–10
52
53
54
55
56
57
58
59
60

1
2
3 min = 100% B; and 10.01–12 min = 5% B.
4
5
6
7

8 Ionization of chromatographic eluates was induced on the QTOF/MS using an ESI source in the
9 positive mode operated under the following conditions: gas temperature at 225°C; sheath gas
10 temperature at 350°C; drying gas flow at 14 L/min; sheath gas flow at 11 L/min; nebulizer
11 pressure at 40 psig; voltage cap at 3000 V; and nozzle voltage at 500 V. Data acquisition was run
12 at 2GHz in extended dynamic range mode. Both TOF/MS and MS/MS spectra were collected in
13 automated MS/MS mode using 500 arbitrary units as threshold for inducing MS/MS data
14 collection. An active exclusion was used after 1 spectra, with a release time of 0.05 min. Each
15 sample was run in triplicate.
16
17
18
19
20
21
22
23
24
25
26
27

28 To detect the analyte of interest and any impurities, the total ion chromatogram (TIC) obtained
29 from the LC-QTOF/MS run was analyzed using Agilent MassHunter Qualitative Analysis
30 software (Agilent Technologies, Sta. Clara, CA). A search was done using the chemical formula
31 of the expected material to confirm the identity and measure retention time of the major
32 chromatogram peak. To confirm, the following criteria were imposed for a compound match:
33 mass error ≤ 10 ppm; target score ≥ 70 (indication of mass and isotopic pattern matches) for
34 peaks that did not exhibit detector saturation; and the presence of at least one expected fragment
35 ion peak in its MS/MS spectra. MS/MS spectra were captured to assess the unique fragmentation
36 of each parent cannabinoid.
37
38
39
40
41
42
43
44
45
46
47
48
49
50

51 ***In vitro* cannabinoid receptor binding experiments.** Experiments utilized human CB₁ or CB₂
52 tagged at the *N*-terminus with three haemagglutinin sequences (HA-hCB₁, HA-hCB₂) stably
53
54
55
56
57
58
59
60

1
2
3 transfected into HEK 293^{22,23}. HEK 293 were cultivated in Dulbecco's Modified Eagle's
4 Medium (DMEM) supplemented with 10% fetal bovine serum (FBS) and zeocin, (250 µg/mL).
5
6 Cells were maintained in 5% CO₂ at 37 °C in a humidified atmosphere. Cells were grown in 75
7
8 mm² flasks and passaged when 80-90% confluent.
9

10
11
12
13
14 HEK 293-hCB₁ or HEK293-hCB₂ cells were grown to 90–100% confluence in 175 cm² flasks
15
16 and harvested in ice-cold phosphate buffered saline (PBS) with 5 mM EDTA. Cells were
17
18 centrifuged at 200 × g for 10 minutes and the pellet frozen at –80 °C until required. Pellets were
19
20 thawed with Tris-sucrose buffer (50 mM Tris-HCl, pH 7.4, 200 mM sucrose, 5 mM MgCl₂, 2.5
21
22 mM EDTA) and homogenized with a glass homogenizer. The homogenate was centrifuged at
23
24 1000 × g for 10 minutes at 4 °C and the pellet discarded. The supernatant was then centrifuged at
25
26 27 000 × g for 30 minutes at 4 °C. The final pellet was resuspended in a minimal volume of Tris-
27
28 sucrose buffer, and aliquoted then stored at –80 °C. Protein concentration was determined using
29
30 the DC protein assay kit (Bio-Rad, Hercules, CA, USA) following the manufacturers protocol.
31
32
33 Initial compound screening involved resuspending cell membranes (5 µg/point) in binding buffer
34
35 (50 mM HEPES, 1 mM MgCl₂, 1 mM CaCl₂, 0.2% (w/v) bovine serum albumin (BSA, ICP
36
37 Bio, New Zealand, pH 7.4) and incubating with [³H]SR141716A (1.25 nM) for CB₁ or
38
39 [³H]CP55,940 (1.0 nM) for CB₂ (PerkinElmer, Waltham, MA, USA; specific activity) and 10
40
41 µM of the test compound at 30 °C for 60 minutes. GF/C Harvest Plates (PerkinElmer) were pre-
42
43 soaked in 0.1% polyethylenimine for one hour and then washed with 200 µL ice cold wash
44
45 buffer (50 mM HEPES pH 7.4 500 mM NaCl, 0.1 % BSA) prior to filtration of samples, which
46
47 were then subject to 3 additional 200 µL washes in ice cold wash buffer. Harvest plates were
48
49 dried overnight at 24 °C, then 50 µL of scintillation fluid (Irgasafe Plus; PerkinElmer) was added
50
51
52
53
54
55
56
57
58
59
60

1
2
3 to each well and plates were read 30 minutes later for 2 minutes per well in a Microbeta Trilux
4 (PerkinElmer). Screening assays were performed in duplicate, repeating assays for each mediator
5
6 (PerkinElmer). Screening assays were performed in duplicate, repeating assays for each mediator
7
8 3 or more times. Non-specific binding was defined as binding that occurred in the presence of
9
10 10 μM CP 55,940. Compounds that produced $>60\%$ displacement at 10 μM were further
11
12 characterized to define affinity. Concentration response curves were carried out by incubating
13
14 the membranes and radioligand with a range of concentrations of test compound. Data was
15
16 analyzed using GraphPad Prism, curves are generated using a One site-fit K_i Competitive
17
18 Binding function with K_d of [^3H]SR141716A constrained to 1.0 nM at CB_1 , and [^3H]CP 55,940
19
20 at 1.0 nM at CB_2 .
21
22
23
24
25

26 ***In vitro* cannabinoid receptor functional activity assay.** Mouse AtT20 neuroblastoma cells
27
28 stably transfected with human CB_1 or human CB_2 have been previously described,²⁴ and were
29
30 cultured in Dulbecco's modified Eagle's medium (DMEM) containing 10% fetal bovine serum
31
32 (FBS), 100 U penicillin/streptomycin, and 80 mg/ml hygromycin. Cells were passaged at 80%
33
34 confluency as required. Cells for assays were grown in 75 cm^2 flasks and used at 90%
35
36 confluence. The day before the assay cells were detached from the flask with trypsin/EDTA
37
38 (Sigma) and resuspended in 10 mL of Leibovitz's L-15 media supplemented with 1% FBS, 100
39
40 U penicillin/streptomycin and 15 mM glucose. The cells were plated in volume of 90 μL in black
41
42 walled, clear bottomed 96-well microplates (Corning) which had been precoated with poly-L-
43
44 lysine (Sigma, Australia). Cells were incubated overnight at 37 $^\circ\text{C}$ in ambient CO_2 .
45
46
47
48
49
50

51 Membrane potential was measured using a FLIPR Membrane Potential Assay kit (blue) from
52
53 Molecular Devices, as described previously.²⁵ The dye was reconstituted with assay buffer of
54
55
56
57
58
59
60

1
2
3 composition (mM): NaCl 145, HEPES 22, Na₂HPO₄ 0.338, NaHCO₃ 4.17, KH₂PO₄ 0.441,
4
5 MgSO₄ 0.407, MgCl₂ 0.493, CaCl₂ 1.26, glucose 5.56 (pH 7.4, osmolarity 315 ± 5). Prior to the
6
7 assay, cells were loaded with 90 μL/well of the dye solution without removal of the L-15, giving
8
9 an initial assay volume of 180 μL/well. Plates were then incubated at 37 °C at ambient CO₂ for
10
11 45 min. Fluorescence was measured using a FlexStation 3 (Molecular Devices) microplate reader
12
13 with cells excited at a wavelength of 530 nm and emission measured at 565 nm. Baseline
14
15 readings were taken every 2 s for at least 2 min, at which time either drug or vehicle was added
16
17 in a volume of 20 μL. The background fluorescence of cells without dye or dye without cells was
18
19 negligible. Changes in fluorescence were expressed as a percentage of baseline fluorescence
20
21 after subtraction of the changes produced by vehicle addition, which was less than 2% for drugs
22
23 dissolved in assay buffer or DMSO. The final concentration of DMSO was not more than 0.1%.
24
25
26
27
28
29
30

31 Data were analyzed with PRISM (GraphPad Software Inc., San Diego, CA), using four-
32
33 parameter nonlinear regression to fit concentration-response curves. In all plates, a maximally
34
35 effective concentration of CP 55,940 was added to allow for normalization between assays.
36
37
38
39

40 ***In vivo* pharmacological assessment of 5F-CUMYL-P7AICA.** Four adult male (C57BL/6J)
41
42 mice (Animal Resources Centre, Perth, Australia) were used for biotelemetric assessment of
43
44 body temperature following 5F-CUMYL-P7AICA administration. Initially, mice weighed
45
46 between 21.2 and 29.5 g. The mice were singly housed in a climate-controlled testing room (23 ±
47
48 1 °C) on a 12 h light/dark cycle (lights on from 07:00 to 19:00). Water and standard rodent chow
49
50 were provided ad libitum. All experiments were approved by The University of Sydney Animal
51
52 Ethics Committee.
53
54
55
56
57
58
59
60

1
2
3
4
5 Biotelemetry transmitters (TA-F10, Data Sciences International, St. Paul, MN) were implanted
6
7 as according to manufacturer instructions. Briefly, the transmitter was implanted according to the
8
9 manufacturers protocol into the peritoneal cavity following anaesthization with isoflurane (3%
10
11 induction, 1–2% maintenance). The wound was sutured closed and data collection commenced
12
13 after 10 days of recovery.
14
15
16
17
18

19 The mice were habituated over multiple days to intraperitoneal injections of vehicle (a solution
20
21 composed of 7.8% polysorbate 80 and 92.2% physiological saline). Injection always occurred at
22
23 a set time of day (10:00 am). The final vehicle habituation injection was used as a drug-free
24
25 baseline, to which all drug doses were compared. The mice received injections of 5F-CUMYL-
26
27 P7AICA in an ascending dose sequence (0.1, 0.3, 1, and 3 mg/kg). This ascending sequence was
28
29 used in order to minimize the risk posed to the animals in assessing hitherto untested compounds.
30
31 Two washout (drug-free) days were given between each dose to limit development of tolerance.
32
33
34
35
36
37

38 Antagonist testing was performed similarly, using four additional drug-naïve mice. The mice
39
40 were implanted with biotelemetry transmitters, habituated to injections, and then pre-treated with
41
42 either 10 mg/kg CB1-receptor selective antagonist SR141716 (rimonabant) or vehicle (counter-
43
44 balanced). Antagonist pre-treatment was given 30 min prior to 1 mg/kg 5F-CUMYL-P7AICA
45
46 injections. A vehicle-vehicle baseline (one vehicle pre-treatment followed by another vehicle
47
48 injection) was used as baseline.
49
50
51
52
53
54
55
56
57
58
59
60

1
2
3 Body temperature data was gathered continuously at 1000 Hz and organized into 15 minute bins
4
5 using Dataquest A.R.T. software (version 4.3, Data Sciences International, St. Paul, MN), and
6
7 analysed using PRISM (Graphpad Software Inc., San Diego, CA).
8
9

10
11
12 **Results and discussion.** The synthesis of **5** is shown in Figure 3, while the synthesis of **6** and **7**
13
14 is shown in Figure 4. Using a convenient one-pot procedure, indole (**8**) was first alkylated with
15
16 1-bromo-5-fluoropentane, and then converted to the corresponding 3-trifluoroacetylidole (**9**) by
17
18 trifluoroacetic anhydride. The crude trifluoroacetylidole intermediate was hydrolyzed to
19
20 carboxylic acid **10**, converted to the corresponding acid chloride using oxalyl chloride, and
21
22 treated with cumylamine to afford 5F-CUMYL-PICA.
23
24
25
26
27

28 [APPROXIMATE PLACEMENT OF FIGURE 3]
29
30
31
32

33 The synthesis of **6** and **7** required a slightly different route and is depicted in Figure 3. Methyl
34
35 1*H*-indazole-3-carboxylate (**11**) and methyl pyrrolo[2,3-*b*]pyridine-3-carboxylate (**12**) were
36
37 deprotonated with potassium *tert*-butoxide and treated with 1-bromo-5-fluoropentane to yield the
38
39 desired 1-alkylated indazole-3-carboxylate (**13**) and pyrrolo[2,3-*b*]pyridine-3-carboxylate (**14**)
40
41 esters, respectively. Saponification of **13** and **14** afforded the corresponding acids **15** and **16**,
42
43 which were subsequently coupled with cumylamine using EDC-HOBt to give respective amides
44
45
46
47 **6** and **7**.
48
49
50

51 [APPROXIMATE PLACEMENT OF FIGURE 4]
52
53
54
55
56
57
58
59
60

1
2
3 SCRA**s** **5**, **6**, and **7** were analyzed using ^1H and ^{13}C nuclear magnetic resonance (NMR)
4 spectroscopy. Full details of these analyses are provided in the experimental section. As
5 expected, ^1H NMR spectra for **5**, **6**, and **7** were similar over the chemical shift range of 0-7 ppm,
6 providing few unique signals for conclusive structural differentiation. In the aromatic region of
7 the spectra, however, several unique signals allowed unambiguous discrimination of the
8 heteroaromatic core of each SCRA (Fig. 5). Most notably, the H-2 protons from **5** and **7** were
9 obvious as singlets and shifted to 7.69 ppm and 7.74 ppm relative to trimethylsilane (TMS),
10 respectively. Indazole **6**, containing a nitrogen atom at the 2 position, showed no signal in this
11 region. Indole **5** contained no signals downfield of a multiplet centered on approximately 7.9
12 ppm (H-), while H-4 and H-6 of the 7-azaindole core of **7** were each observed as a doublet of
13 doublets centered on 8.27 ppm and 8.36 ppm, respectively, and with characteristic $^3J_{\text{HH}}$ coupling
14 to H-5 upfield. This is expected for the pyrrolo[2,3-b]pyridine system²⁶ and consistent with a
15 previous ^1H NMR analysis of **7** obtained by isolation from a SCRA NPS product.²⁷ Indazole **6**
16 contained a partially resolved doublet of triplets corresponding to H-4 in the same chemical shift
17 range. Therefore, analysis of the region 7.6 to 8.5 ppm downfield of TMS in the proton NMR
18 spectra should enable simple and rapid discrimination of emergent 7-azaindole-3-carboxamide
19 (7AICA) SCRA**s** from isomeric indazole analogues in future.
20
21
22
23
24
25
26
27
28
29
30
31
32
33
34
35
36
37
38
39
40
41
42
43

44 [APPROXIMATE PLACEMENT OF FIGURE 5]
45
46
47
48

49 In order to provide data of relevance to forensic and clinical toxicologists, synthesized **5**, **6**, and **7**
50 were also analyzed using GC-MS (Fig. 6) and LC-QTOF-MS (Fig. 7). GC-MS/MS spectra for
51 synthesized **5**, **6**, and **7** were obtained independently of Energy Control using a method
52
53
54
55
56
57
58
59
60

1
2
3 developed in our laboratories for the analysis of phytocannabinoids, and some variation in
4 retention time (rt) was expected. The GC–MS total ion chromatograms (TICs) for **5**, **6**, and **7**
5 showed rt of 9.04, 8.09, and 8.52 minutes, respectively, and the MS fragmentation patterns were
6 consistent with those described by Energy Control. Molecular ions were observed by GC–MS for
7 **5** (m/z 366.20), **6** (m/z 367.17), and **7** (m/z 367.16), however, these were generally of low
8 abundance (<20% relative intensity). Although the molecular ion of indole **5** differed from
9 indazole **6** and azaindoles **7** by a single atomic mass unit (amu), the latter are isobaric and could
10 not be distinguished. Similarly, the base peak for each compound corresponded to the acylium
11 ion formed following loss of the cumylamine group and was observed at m/z 232.06 for **5**, and at
12 one greater amu for **6** (m/z 233.06) and **7** (m/z 233.06). Other identifiable peaks include the likely
13 products of a McLafferty rearrangement and subsequent elimination of methylstyrene of **5**, **6**,
14 and **7** at m/z 248.11, 249.09, and 249.08, respectively, as described for related systems.¹⁵ The
15 prominent ion m/z 352.15 observed for **6** corresponds to loss of a single methyl group from the
16 cumylamine side chain, likely due to stabilization of the formed tertiary carbocation, but it is
17 unclear why the corresponding ion was not observed for **5** or **7**. Although **6** could be differentiated
18 from **7** by rt, the mass spectrum fragmentation of these isomers was similar. Therefore, we also
19 analyzed all compounds by LC–QTOF/MS.

20
21
22
23
24
25
26
27
28
29
30
31
32
33
34
35
36
37
38
39
40
41
42
43
44 [APPROXIMATE PLACEMENT OF FIGURE 6]
45
46
47
48

49 The LC–QTOF/MS elution order for **5**, **6**, and **7** paralleled that for GC–MS, with retention times
50 of 6.796, 7.121, and 6.280 minutes, respectively. As shown in Figure 7, protonated molecular
51 ions ($[M + H]^+$) of low abundance were observed for indole **5** (m/z 367.2185, 3.8%, mass error -
52
53
54
55
56
57
58
59
60

1
2
3 0.3 ppm) and indazole **6** (m/z 368.2129, 4.8%, mass error -2.4 ppm), whereas the more basic
4
5 azaindole **7** exhibited a prominent molecular ion (m/z 368.2086, 48.4%, mass error -6.0 ppm). In
6
7 addition to being more facile in the analysis of forensically relevant biological matrices such as
8
9 serum and urine, LC–QTOF/MS provides increased resolution over GC–MS for isobaric
10
11 compounds, demonstrated here for regioisomers **6** and **7**. Examination of the fragmentation
12
13 spectra of **6** and **7** reveal that scaffold-hopping from indazole to the 7-azaindole (1*H*-pyrrolo[2,3-
14
15 *b*]pyridine) core is enough to change the relative abundance of the major fragments of these
16
17 compounds resulting in a reversal of abundances for the fragments m/z 250.13 and m/z 233.10,
18
19 with m/z 250.13 being the base peak for **7** and m/z 233.10 being the base peak for **6**.
20
21 Additionally, **7** is further distinguished by the presence of a unique fragment corresponding to
22
23 m/z 207.13. The only peak that is common to all three compounds is m/z 119.08. The proposed
24
25 fragmentation pathways shown in Figure 7 are entirely consistent with those described
26
27 extensively for **6**, **7**, and related analogues previously.¹⁵
28
29
30
31
32
33
34

35 [APPROXIMATE PLACEMENT OF FIGURE 7]
36
37
38
39

40 The binding affinities and functional activities of **5**, **6**, and **7** at human CB₁ and CB₂ receptors are
41
42 shown in Table 1. As anticipated from their structures and existence on the NPS market, **5**, **6**,
43
44 and **7** all showed affinity for both CB receptor subtypes. Indazole **6** demonstrated the highest
45
46 affinity for CB₁ (K_i = 2.95 nM), while the affinity of indole **5** (K_i = 12.6 nM) was several times
47
48 lower, and that of azaindole **7** (K_i = 174 nM) was an order of magnitude lower again. All SCRA
49
50 also bound to CB₂ (K_i = 0.76–74.9 nM), with affinities approximating those for CB₁ in each
51
52 case.
53
54
55
56
57
58
59
60

[APPROXIMATE PLACEMENT OF TABLE 1]

The trends for functional activities at CB₁ were similar, and all ligands were potent, efficacious agonists, with maximal effects 110–118% of those elicited by 1 μM CP 55,940. Using the same stably transfected cell lines reported by us previously, indazole **6** was a subnanomolar agonist at CB₁ (EC₅₀ = 0.43 nM), followed by indole **5** (EC₅₀ = 2.8 nM), and azaindole **7** (EC₅₀ = 4.7 nM). As with binding, all ligands were also potent and efficacious CB₂ agonists (EC₅₀ = 11.2–39.6 nM). The nanomolar EC₅₀ value for 5F-CUMYL-P7AICA at CB₁ ranks it among other potent SCRAs identified in recent years, like AMB-CHMINACA (CB₁ K_i = 0.339 nM; EC₅₀ = 5.1 nM) and MDMB-FUBINACA (CB₁ K_i = 0.0985 nM; EC₅₀ = 3.9 nM), despite demonstrating a binding affinity several orders of magnitude lower than such ligands.^{19,24} The observed affinity and potency trends for the congeneric heteroaromatic series (indazole > indole > 7-azaindole) are consistent with those of SCRAs featuring alternative 1-substituents and different pendant groups in place of cumylamine.^{17,24,28}

The cannabimimetic activity of 5F-CUMYL-PICA in rats was recently reported^{17,20}. However, it is not currently known whether the 7-azaindole core of 5F-CUMYL-P7AICA confers cannabinoid activity *in vivo*. This is especially important due to the difference between CB₁ affinity and functional activity reported above for this SCRA. To address this question, the hypothermic effects of 5F-CUMYL-P7AICA in mice were assessed using biotelemetry.

1
2
3 5F-CUMYL-P7AICA produced clear hypothermia in mice when injected intraperitoneally at 0.3
4 mg/kg or higher (Figure 8a). This hypothermic effect was brief, lasting approximately 1 h
5
6
7 irrespective of dose. A dose of 3 mg/kg caused profound hypothermia, where body temperature
8
9
10 fell approximately 6 °C below baseline. Additionally, pre-treatment with 10 mg/kg SR141716
11
12 (rimonabant) blocked the hypothermia elicited by 1 mg/kg 5F-CUMYL-P7AICA, pointing to a
13
14 CB₁ receptor mediated mechanism, in agreement with *in vitro* CB₁ receptor activity (Figure 8b).
15
16
17 Taken together with the *in vitro* data, biotelemetry suggests that binding affinity alone is not
18
19 sufficient to predict the *in vivo* potency of new SCRAs.
20
21
22
23

24 [APPROXIMATE PLACEMENT OF FIGURE 8]
25
26
27

28 **Conclusion.** Although the earliest SCRA NPS were repurposed compounds found in the
29
30 chemical literature, recent structures are often unknown prior to first detection in the NPS
31
32 market, and often appear to be the products of rational design using medicinal chemistry
33
34 techniques such as scaffold hopping. Synthetic methods for preparation of reference standards
35
36 for scaffold hopping SCRAs 5F-CUMYL-PICA, 5F-CUMYL-PINACA, 5F-CUMYL-P7AICA
37
38 was developed, and these methods should be general for related carboxamide SCRAs featuring
39
40 indole, indazole, and 7-azaindole cores. 5F-CUMYL-PICA, 5F-CUMYL-PINACA, 5F-
41
42 CUMYL-P7AICA were differentiated by GC-MS, and more easily by LC-QTOF-MS, due to
43
44 differences in fragmentation patterns in both modalities. Despite similar structures, these SCRAs
45
46 showed dramatic differences in CB₁ binding affinity, with the 7-azaindole core of 5F-CUMYL-
47
48 P7AICA conferring reduced affinity and functional activity compared to the indazole or indole
49
50 cores of 5F-CUMYL-PINACA and 5F-CUMYL-PICA, respectively. Despite this, 5F-CUMYL-
51
52
53
54
55
56
57
58
59
60

1
2
3 P7AICA demonstrated potent hypothermic effects in mice through a CB₁-dependent mechanism,
4
5 confirming the activity of this SCRA *in vivo*. Since scaffold hopping from indole or indazole to
6
7 the corresponding 7-azaindole does not abolish the cannabimimetic activity of the cumylamine-
8
9 carboxamide class of SCRA, we anticipate that this heterocycle will continue to appear as a
10
11 replacement for indole and indazole cores in emergent SCRA NPS.
12
13
14
15
16
17
18
19
20
21
22
23
24
25
26
27
28
29
30
31
32
33
34
35
36
37
38
39
40
41
42
43
44
45
46
47
48
49
50
51
52
53
54
55
56
57
58
59
60

For Peer Review

References.

1. United Nation Office on Drugs and Crime. World Drug Report 2017. United Nations publication, Sales No. E.17.XI.6, 2017. Available at <http://www.unodc.org/wdr2017>. Accessed 31 January 2018.
2. Langer N, Lindigkeit R, Schiebel HM, Papke U, Ernst L, Beuerle T. Identification and quantification of synthetic cannabinoids in "spice-like" herbal mixtures: Update of the German situation for the spring of 2016. *Forensic Sci Int.* 2016;269:31-41. <https://doi.org/10.1016/j.forsciint.2016.10.023>.
3. Adams AJ, Banister SD, Irizarry L, Trecki J, Schwartz M, Gerona R. "Zombie" outbreak caused by the synthetic cannabinoid AMB-FUBINACA in New York. *New Engl J Med.* 2017;376(3):235-242. <https://doi.org/10.1056/NEJMoa1610300>.
4. Angerer V, Mogler L, Steitz JP, et al. Structural characterization and pharmacological evaluation of the new synthetic cannabinoid CUMYL-PEGACLONE. *Drug Test Anal.* 2018;10(3):597-603. <https://doi.org/10.1002/dta.2237>.
5. Asada A, Doi T, Tagami T, et al. Cannabimimetic activities of cumyl carboxamide-type synthetic cannabinoids. *Forensic Toxicol.* 2017;36(1):170-177. <https://doi.org/10.1007/s11419-017-0374-9>.
6. Dobaja M, Grenc D, Kozelj G, Brvar M. Occupational transdermal poisoning with synthetic cannabinoid cumyl-PINACA. *Clin Toxicol.* 2017;55(3):193-195. <https://doi.org/10.1080/15563650.2016.1278224>.
7. Staeheli SN, Poetzsch M, Veloso VP, et al. In vitro metabolism of the synthetic cannabinoids CUMYL-PINACA, 5F-CUMYL-PINACA, CUMYL-4CN-BINACA, 5F-

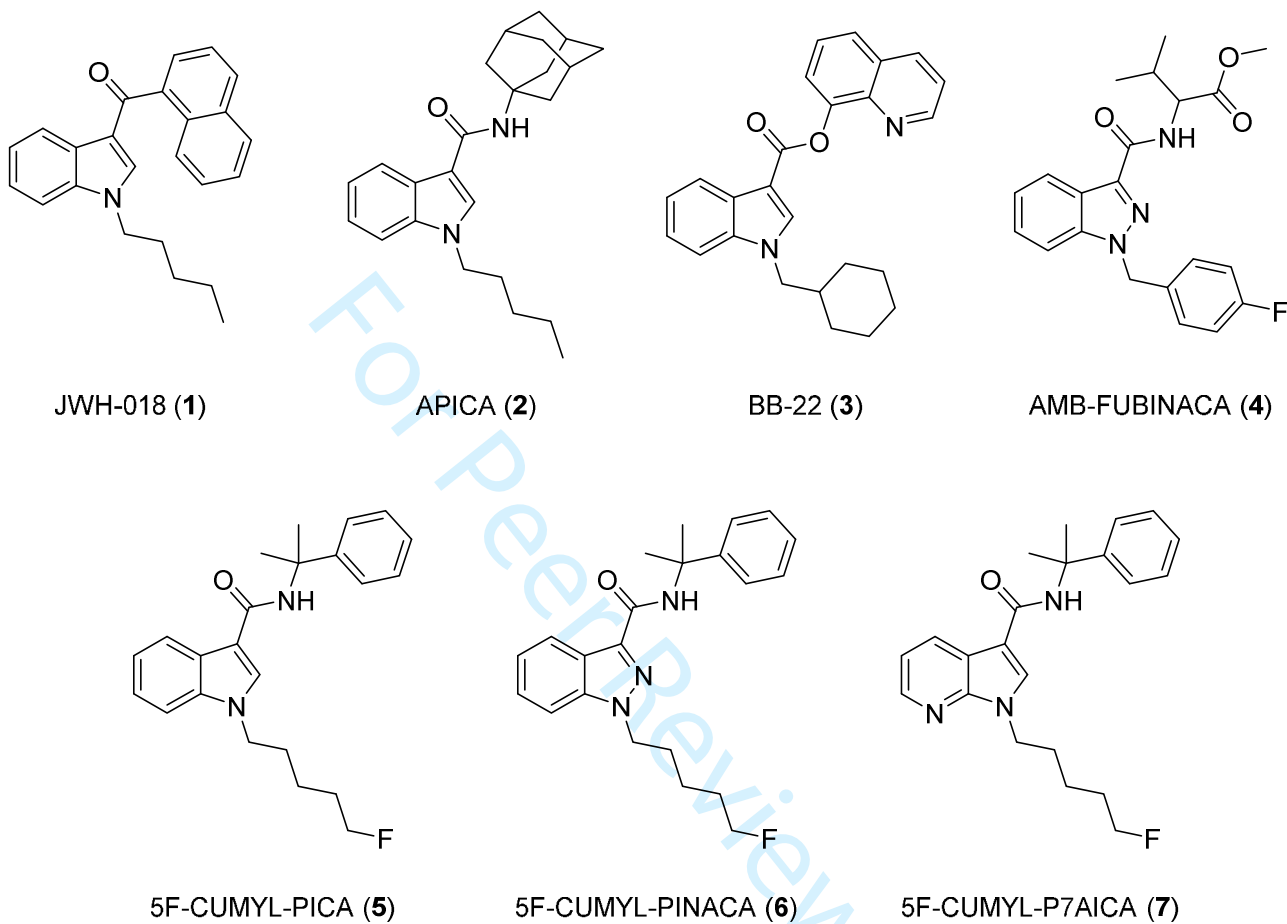
- 1
2
3 CUMYL-P7AICA and CUMYL-4CN-B7AICA. *Drug Test Anal.* 2018;10(1):148-157.
4
5 <https://doi.org/10.1002/dta.2298>.
6
7
8 8. European Monitoring Centre for Drugs and Drug Addiction. EMCDDA–Europol 2014
9
10 Annual Report on the implementation of Council Decision 2005/387/JHA. Publications
11
12 Office of the European Union, Luxembourg, 2015. <https://doi.org/10.2810/112317>.
13
14
15 9. Bowden MJ, Williamson JPB. Preparation of cannabinoid indole and indazole
16
17 compounds for treating pain and nausea, stimulating appetite, and inducing a positive
18
19 mood change. World patent 2014167530.
20
21
22 10. European Monitoring Centre for Drugs and Drug Addiction. EMCDDA–Europol 2015
23
24 Annual Report on the implementation of Council Decision 2005/387/JHA. Publications
25
26 Office of the European Union, Luxembourg, 2016. <https://doi.org/10.2810/932574>.
27
28
29 11. Bohm HJ, Flohr A, Stahl M. Scaffold hopping. *Drug Discov Today Technol.*
30
31 2004;1(3):217-224. <https://doi.org/10.1016/j.ddtec.2004.10.009>.
32
33
34 12. Sun H, Tawa G, Wallqvist A. Classification of scaffold-hopping approaches. *Drug*
35
36 *Discov Today.* 2012;17(7–8):310-324. <https://doi.org/10.1016/j.drudis.2011.10.024>.
37
38
39 13. Blaazer AR, Lange JH, van der Neut MA, et al. Novel indole and azaindole
40
41 (pyrrolopyridine) cannabinoid (CB) receptor agonists: design, synthesis, structure-
42
43 activity relationships, physicochemical properties and biological activity. *Eur J Med*
44
45 *Chem.* 2011;46(10):5086-5098. <https://doi.org/10.1016/j.ejmech.2011.08.021>.
46
47
48 14. Qian Z, Jia W, Li T, Hua Z, Liu C. Identification and analytical characterization of four
49
50 synthetic cannabinoids ADB-BICA, NNL-1, NNL-2, and PPA(N)-2201. *Drug Test Anal.*
51
52 2017;9(1):51-60. <https://doi.org/10.1002/dta.1990>.
53
54
55
56
57
58
59
60

- 1
2
3 15. Bovens M, Bissig C, Staeheli SN, Poetzsch M, Pfeiffer B, Kraemer T. Structural
4 characterization of the new synthetic cannabinoids CUMYL-PINACA, 5F-CUMYL-
5 PINACA, CUMYL-4CN-BINACA, 5F-CUMYL-P7AICA and CUMYL-4CN-B7AICA.
6
7
8
9
10
11
12
13 16. Liu C, Jia W, Hua Z, Qian Z. Identification and analytical characterization of six
14 synthetic cannabinoids NNL-3, 5F-NPB-22-7N, 5F-AKB-48-7N, 5F-EDMB-PINACA,
15 EMB-FUBINACA, and EG-018. *Drug Test Anal.* 2017;9(8):1251-1261.
16
17
18
19
20
21
22 17. Longworth M, Banister SD, Boyd R, et al. Pharmacology of cumyl-carboxamide
23 synthetic cannabinoid new psychoactive substances (NPS) CUMYL-BICA, CUMYL-
24 PICA, CUMYL-5F-PICA, CUMYL-5F-PINACA, and their analogues. *ACS Chem*
25
26
27
28
29
30
31 18. Gamage TF, Farquhar CE, Lefever TW, et al. Molecular and behavioral pharmacological
32 characterization of abused synthetic cannabinoids MMB- and MDMB-FUBINACA, MN-
33 18, NNEI, CUMYL-PICA, and 5-Fluoro-CUMYL-PICA. *J Pharmacol Exp Ther.*
34
35
36
37
38
39
40 19. Schoeder CT, Hess C, Madea B, Meiler J, Müller CE. Pharmacological evaluation of new
41 constituents of “Spice”: synthetic cannabinoids based on indole, indazole, benzimidazole
42 and carbazole scaffolds. *Forensic Toxicol.* 2018 (in press).
43
44
45
46
47
48
49 20. Kevin RC, Lefever TW, Snyder RW, et al. In vitro and in vivo pharmacokinetics and
50 metabolism of synthetic cannabinoids CUMYL-PICA and 5F-CUMYL-PICA. *Forensic*
51
52
53
54
55
56
57
58
59
60

- 1
2
3 21. Banister SD, Stuart J, Kevin RC, et al. Effects of bioisosteric fluorine in synthetic
4 cannabinoid designer drugs JWH-018, AM-2201, UR-144, XLR-11, PB-22, 5F-PB-22,
5 APICA, and STS-135. *ACS Chem Neurosci*. 2015;6(8):1445-1458.
6 <https://doi.org/10.1021/acschemneuro.5b00107>.
7
8
9
10
11
12 22. Finlay DB, Cawston EE, Grimsey NL, et al. Gas signalling of the CB1 receptor and the
13 influence of receptor number. *Br J Pharmacol*. 2017;174(15):2545-2562.
14 <https://doi.org/10.1111/bph.13866>.
15
16
17
18
19 23. Grimsey NL, Goodfellow CE, Dragunow M, Glass M. Cannabinoid receptor 2 undergoes
20 Rab5-mediated internalization and recycles via a Rab11-dependent pathway. *Biochim*
21 *Biophys Acta*. 2011;1813(8):1554-1560. <https://doi.org/10.1016/j.bbamcr.2011.05.010>.
22
23
24
25
26 24. Banister SD, Longworth M, Kevin R, et al. Pharmacology of valinate and tert-leucinate
27 synthetic cannabinoids 5F-AMBICA, 5F-AMB, 5F-ADB, AMB-FUBINACA, MDMB-
28 FUBINACA, MDMB-CHMICA, and their analogues. *ACS Chem Neurosci*.
29 2016;7(9):1241-1254. <https://doi.org/10.1021/acschemneuro.6b00137>.
30
31
32
33
34
35 25. Knapman A, Santiago M, Du YP, Bennallack PR, Christie MJ, Connor M. A continuous,
36 fluorescence-based assay of mu-opioid receptor activation in AtT-20 cells. *J Biomol*
37 *Screen*. 2013;18(3):269-276. <https://doi.org/10.1177/1087057112461376>.
38
39
40
41
42 26. Cox RH, Sankar S. 1H and 13C NMR studies of 7-azaindole and related compounds. *Org*
43 *Mag Res*. 1980;14(2):150-152. <https://doi.org/10.1002/mrc.1270140216>.
44
45
46
47 27. Ernst L, Brandhorst K, Papke U, et al. Identification and quantification of synthetic
48 cannabinoids in 'spice-like' herbal mixtures: Update of the German situation in early
49 2017. *Forensic Sci Int*. 2017;277:51-58. <https://doi.org/10.1016/j.forsciint.2017.05.019>.
50
51
52
53
54
55
56
57
58
59
60

- 1
2
3 28. Banister SD, Moir M, Stuart J, et al. Pharmacology of indole and indazole synthetic
4 cannabinoid designer drugs AB-FUBINACA, ADB-FUBINACA, AB-PINACA, ADB-
5 PINACA, 5F-AB-PINACA, 5F-ADB-PINACA, ADBICA, and 5F-ADBICA. *ACS Chem*
6 *Neurosci.* 2015;6(9):1546-1559. <https://doi.org/10.1021/acchemneuro.5b00112>.
7
8
9
10
11
12
13
14
15
16
17
18
19
20
21
22
23
24
25
26
27
28
29
30
31
32
33
34
35
36
37
38
39
40
41
42
43
44
45
46
47
48
49
50
51
52
53
54
55
56
57
58
59
60

For Peer Review

Figures and Tables.**Figure 1.** Selected synthetic cannabinoid receptor agonist (SCRA) new psychoactive substances (NPS).

1
2
3 **Figure 2.** (a) Packaging of “Rasta King” product obtained by test purchase, and (b) GC-MS TIC
4 and fragmentation spectrum of 5F-CUMYL-P7AICA detected in “Rasta King” by Energy
5
6 and fragmentation spectrum of 5F-CUMYL-P7AICA detected in “Rasta King” by Energy
7
8 Control.

9
10 **(a)**



32 **(b)**

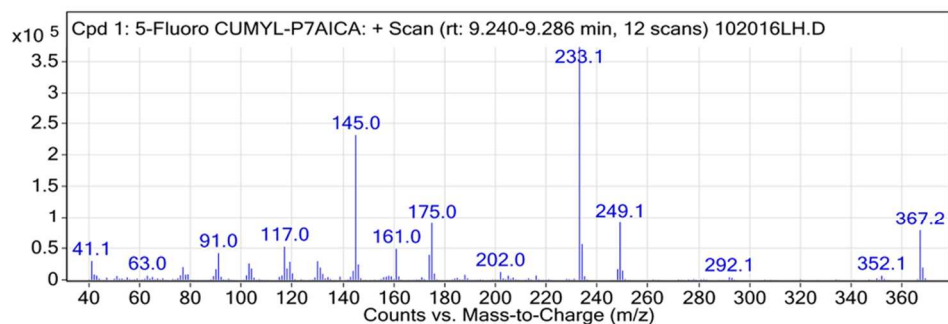
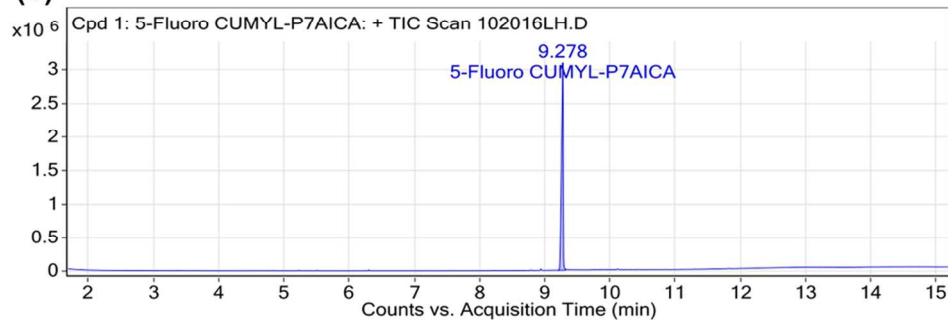


Figure 3. Reagents and conditions: (a)(i) NaH, Br(CH₂)₅F, DMF, 0 °C–rt, 1 h; (ii) (CF₃CO)₂O, 0 °C–rt, 1 h; (b) KOH, MeOH, PhMe, reflux, 2 h, 67% over 3 steps; (c) (COCl)₂, DMF (cat.), CH₂Cl₂, 0 °C–rt, 2 h; (d) PhC(CH₃)₂NH₂, Et₃N, CH₂Cl₂, 0 °C–rt, 14 h, 78%.

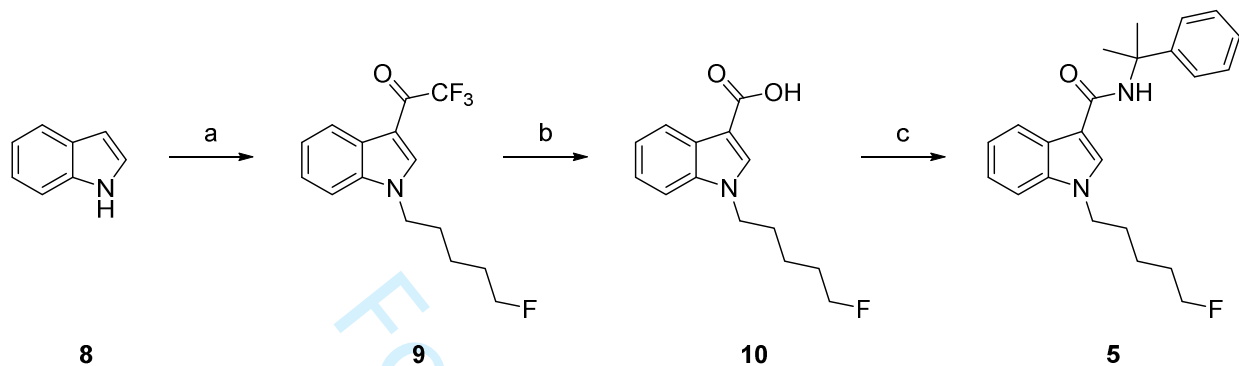


Figure 4. Reagents and conditions: (a) KO^tBu , $\text{F}(\text{CH}_2)_5\text{Br}$, THF, $0\text{ }^\circ\text{C}$ –rt, 14 h, (**13**: 78%; **14**: 66%); (b) 1 M aq. NaOH, MeOH, rt, 16 h, (**15**: 98%; **16**: 94%); (c) EDC·HCl, HOBT·H₂O, $\text{PhC}(\text{CH}_3)_2\text{NH}_2$, Et₃N, DMF, rt, 13 h, 90% (**6**: 82%; **7**: 81%).

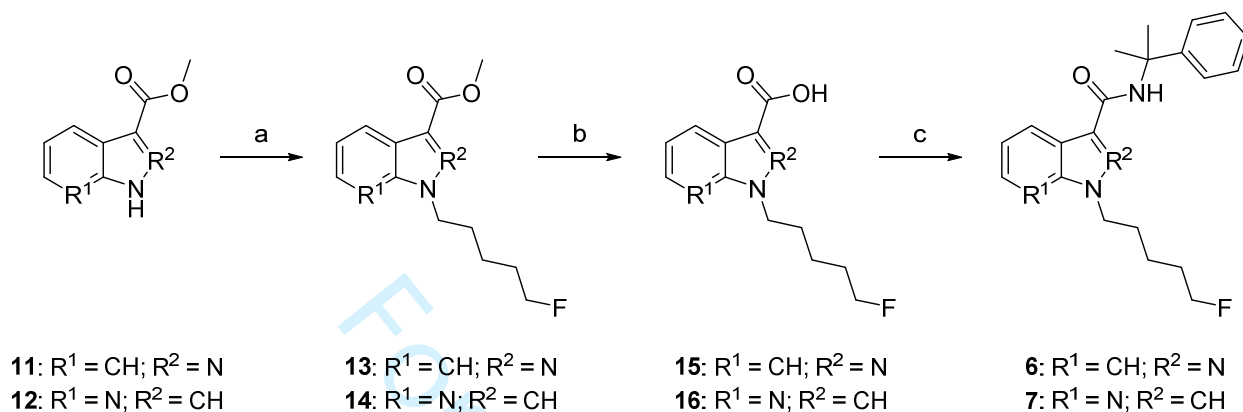


Figure 5. Expansions of the aromatic regions of the ^1H NMR (400 MHz, CDCl_3) spectra for (a) **5**, (b) **6**, and (c) **7**. All spectra calibrated to residual CHCl_3 (δ 7.26 ppm).

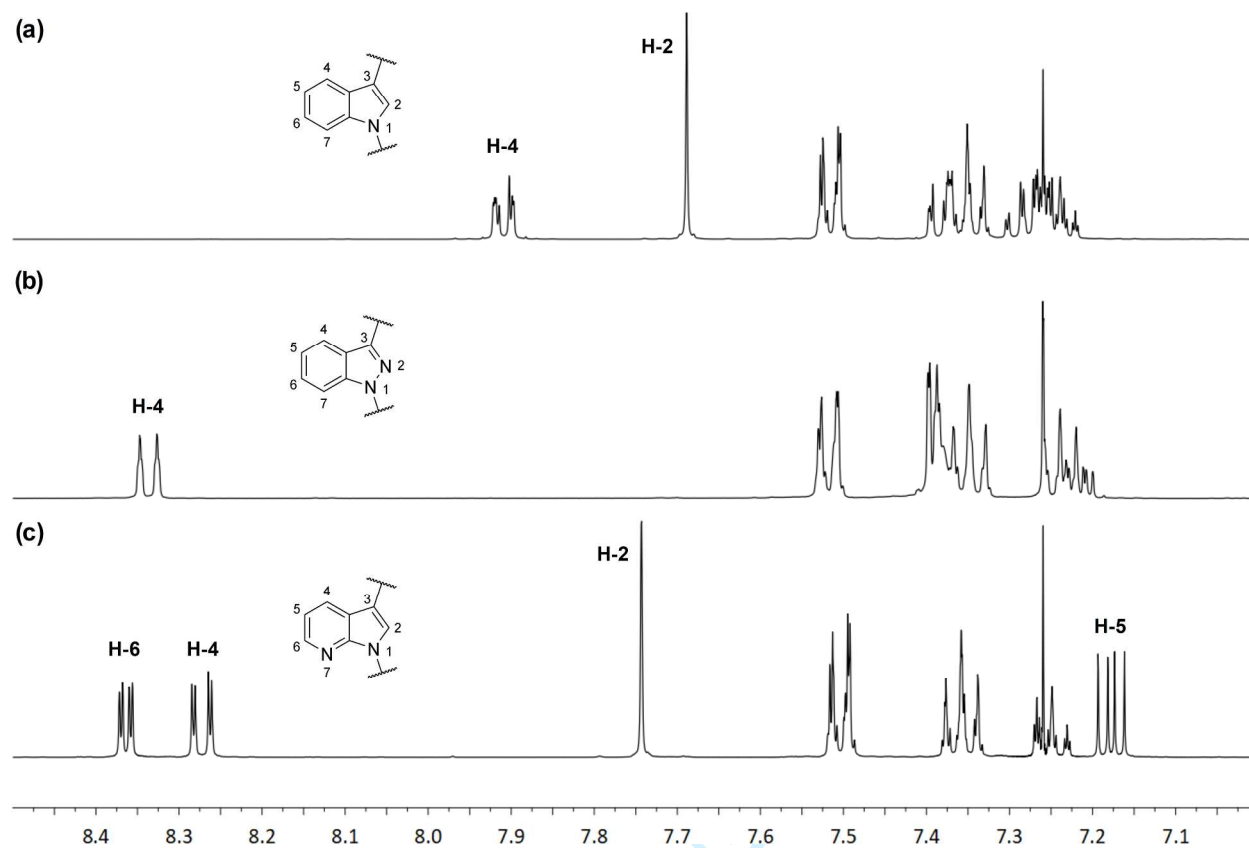


Figure 6. GC-MS ESI mass spectra fragmentation for (a) 5F-CUMYL-PICA, (b) 5F-CUMYL-PINACA, and (c) 5F-CUMYL-P7AICA.

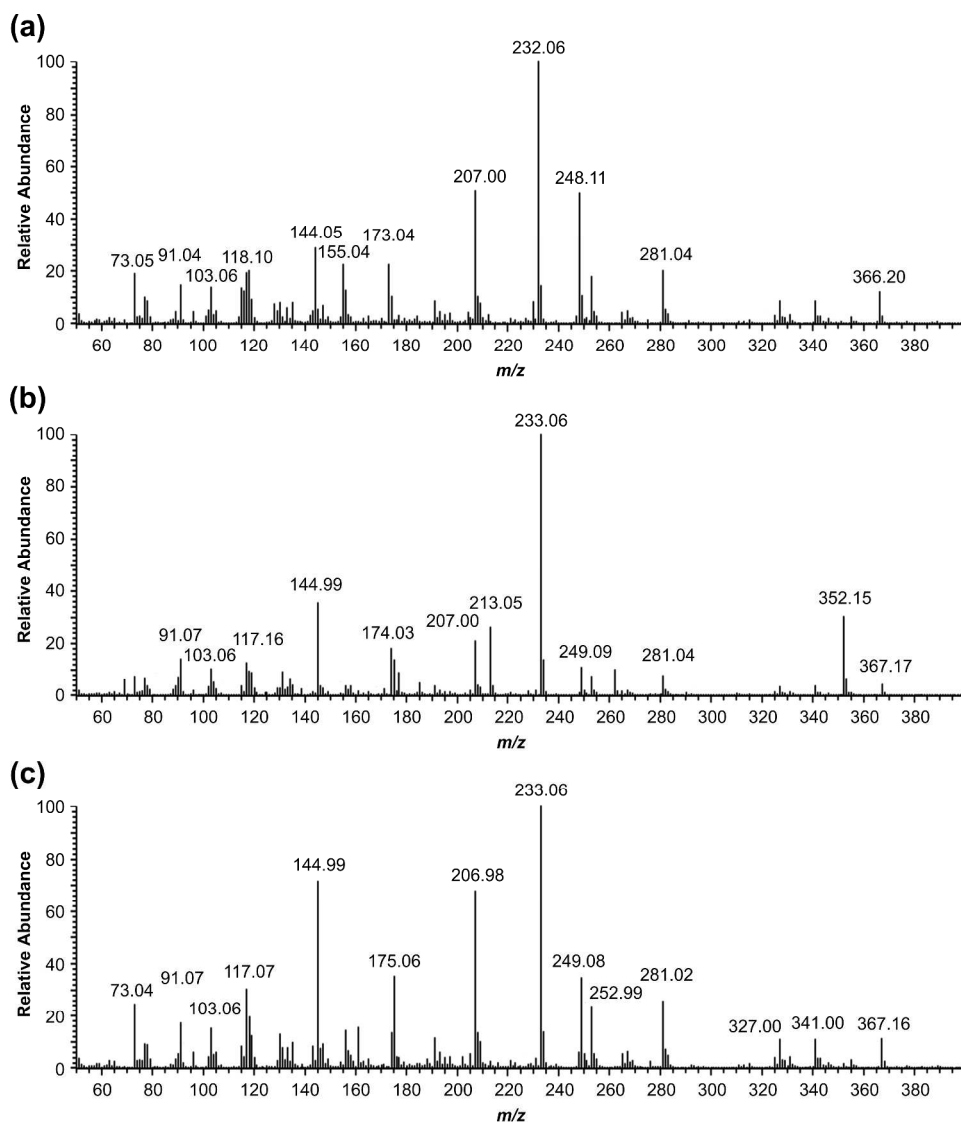


Figure 7. LC-QTOF-MS mass spectra and proposed fragmentations for (a) 5F-CUMYL-PICA, (b) 5F-CUMYL-PINACA, and (c) 5F-CUMYL-P7AICA.

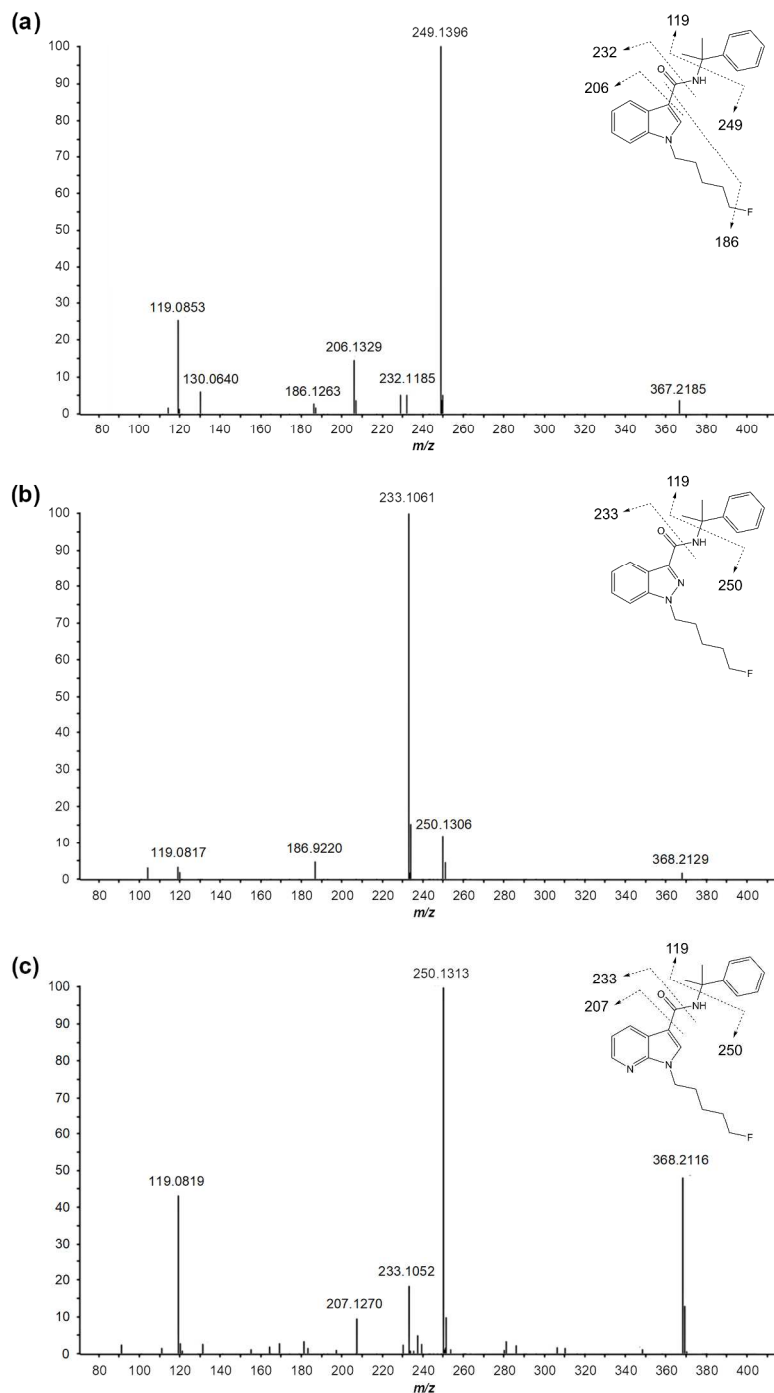


Figure 8. Mice body temperature following intraperitoneal injection (dashed line) of (a) 5F-CUMYL-P7AICA and (b) 1 mg/kg 5F-CUMYL-P7AICA following pre-treatment with either drug-free vehicle solution or with 10 mg/kg SR141716 (rimonabant). All shown as difference from drug-free baseline injections (mean \pm SEM; n = 4).

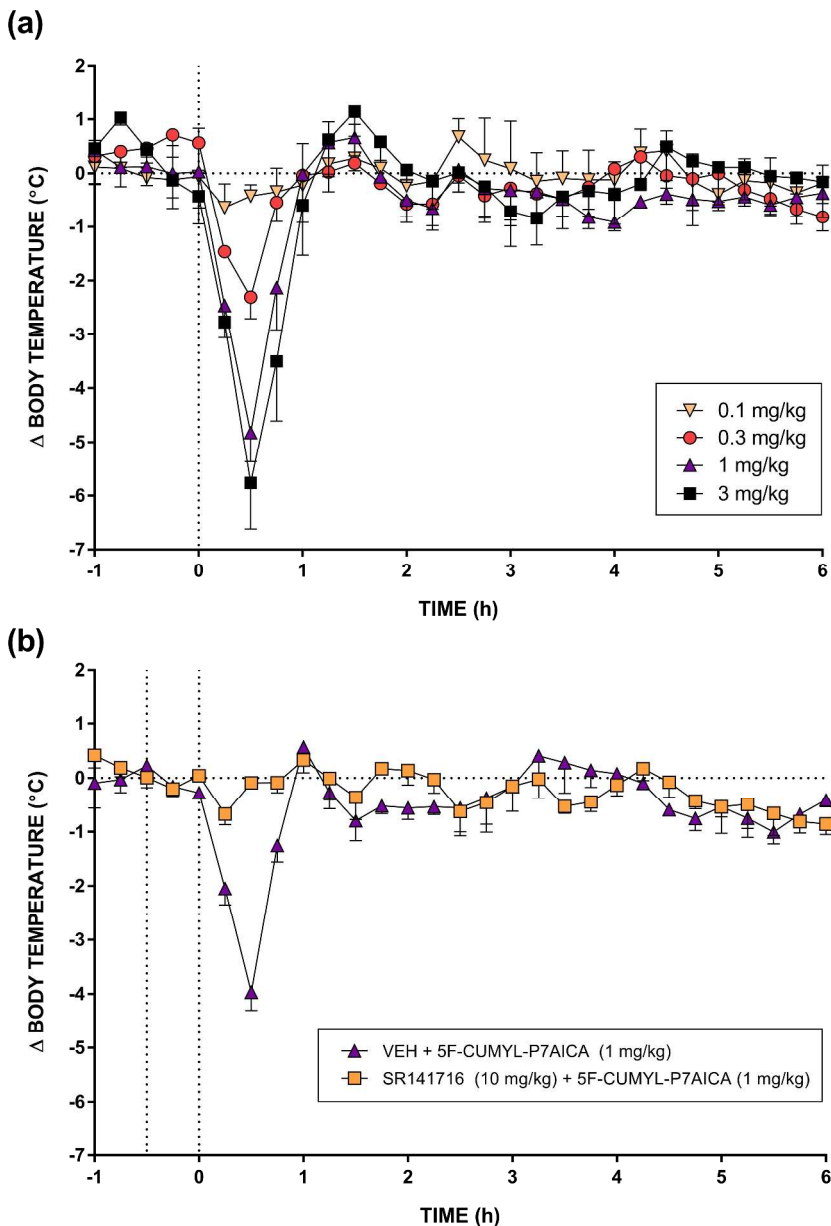


Table 1. Binding affinities and functional activities of SCRA 5, 6, and 7 at hCB₁ and hCB₂ receptors.

Compound	hCB ₁			hCB ₂		
	pK_i ± SEM (K_i, nM)	pEC₅₀ ± SEM (EC₅₀, nM)	Max ± SEM (% CP 55,940)	pK_i ± SEM (K_i, nM)	pEC₅₀ ± SEM (EC₅₀, nM)	Max ± SEM (% CP 55,940)
5F-CUMYL-PICA (5)	7.90 ± 0.09 (12.6)	8.55 ± 0.05 (2.8) ^a	118 ± 2 ^a	7.86 ± 0.08 (13.8)	7.40 ± 0.10 (39.6) ^a	104 ± 5 ^a
5F-CUMYL-PINACA (6)	8.53 ± 0.04 (2.95)	9.37 ± 0.06 (0.43) ^a	110 ± 3 ^a	9.12 ± 0.12 (0.76)	7.95 ± 0.09 (11.2) ^a	87 ± 3 ^a
5F-CUMYL-P7AICA (7)	6.76 ± 0.18 (174)	8.33 ± 0.05 (4.7)	110 ± 3	7.12 ± 0.14 (75.9)	7.95 ± 0.09 (11.3)	90 ± 3

^aData extracted from reference 17.